Design and characterisation of auxetic lattice with controlled transitions to near-zero Poisson's ratio

Mokaddemul Islam Asha[1*], *Perk Lin* Chong[2], *Hossein* Habibi[2]

[1] PhD researcher, SCEDT, Teesside University, Middlesbrough TS1 3BX, UK.

[2] Professor, SCEDT, Teesside University, Middlesbrough TS1 3BX, UK.

Abstract. Auxetic materials, defined by their negative Poisson's ratio, exhibit enhanced toughness, energy absorption, and improved shape retention, making them attractive for aerospace, biomedical, and flexible electronics applications. In contrast, materials with near-zero Poisson's ratio maintain lateral dimensional stability during deformation, which is essential for precision-dependent structures. This study investigates the geometric tuning of Poisson's ratio in porous auxetic lattices through design optimisation. Four configurations, including re-entrant H-based, re-entrant V-shaped, elliptical hole-based, and peanut-shaped hole geometries, were examined by varying key parameters, including the rib inclination angle in re-entrant structures and the rotation angle of elliptical units. ABS samples of consistent dimensions were analysed using finite element simulation. The results reveal a clear relationship between geometric configuration and Poisson's ratio transition behaviour, confirming that small adjustments in inclination or rotation angle can shift the response across negative, near-zero, and positive regimes. Among the structures examined, the elliptical hole-based lattice demonstrated the most stable transition, achieving a near-zero Poisson's ratio at approximately 25.45°, while peanut-shaped geometries showed more abrupt transitions, and re-entrant forms predominantly retained auxetic behaviour. These findings establish inclination angle as a controllable design parameter for tailoring lateral deformation characteristics, supporting the design of multifunctional materials where either auxetic expansion or dimensional stability is required.

[1]Corresponding author: [1]m.asha@tees.ac.uk

1 Introduction

Materials with negative Poisson's ratio (NPR) and zero Poisson's ratio (ZPR) have very special characteristics. To characterize a material's deformation pattern, Poisson's ratio is used. Materials Poisson's ratio and its transition points from negative to positive or from negative to zero are crucial for material properties. A material's Poisson's ratio is a measure of its responsiveness to an applied load or deformation [1]. Poisson's ratio is always between -1 to 0.5 [2]. Negative Poisson's ratio materials, also referred to as auxetic materials, expand laterally when stretched and contract when compressed [3]. Auxetic materials expand with the pulling force and contract with the compression force [4]. Auxetic metamaterials are highly relevant for developing next-generation materials with superior and multifunctional applications [5]. Auxetic structures exhibit higher shear resistance, energy absorption, and indentation resistance, making them useful in protective materials, aerospace, and biomedical applications [6]. One of the key features of negative Poisson's ratio structures is that it is independent of base material stiffness and Poisson's ratio; rather, it is dependent on design optimisation [6]. In contrast to negative Poisson's ratio materials, zero Poisson's ratio materials maintain a constant transverse width when subjected to longitudinal strain [7]. Maintaining dimensional stability under stress enhances stability and accuracy by preventing unwanted deformation, making them unique in mechanical behaviour [8].

Zero Poisson's ratio (ZPR) materials have important applications in the field of precision instruments, because they are stable and not be affected by strain [8]. This feature makes zero ZPR materials extremely rare and have potential applications in the field of precision instruments such as aviation, medicine, and flexible electronics [5]. ZPR materials maintain a constant transverse width when subjected to longitudinal strain [3]. Poisson's ratio of the mechanical metamaterial is closely related to elements geometric structures, the arrangement of elements and the Poisson's ratio of the constituting materials [8]. A hybrid structures can vary between positive & negative by optimizing geometric parameters such as concave angles & features length [8].

Transition points of Poisson's ratio in mechanical metamaterials determine the adaptability in applications requiring variable mechanical response [5]. Therefore, developing materials capable of transitioning between positive and negative Poisson's ratios is achieved through structural reconfiguration and restructuring the material [5]. A Transition points are key for designing adaptive or tuneable materials where Poisson's ratio can be controlled for various applications. At transition point lattice structures undergoes a critical mechanical shift altering how it responds to applied stress.

Although ZPR materials offer significant advantages, a key challenge remains in understanding their transition behaviour under different mechanical conditions. The transition points, where the Poisson's ratio deviates from zero due to factors like materials composition, geometric arrangement and applied stress are not yet fully understood. Therefore, understanding the transition points are crucial for designing materials with tuneable properties for advanced engineering applications.

Studying a full spectrum of Poisson's ratio & transitions will give a comprehensive understanding of how geometric parameters modification influence mechanical behaviour. Many research articles related to NPR, ZPR mechanics, application and auxetic structures design modification explained but transition point of Poisson's ratio of lattice structures by geometric optimisation not investigated thoroughly.

1.1 Feature of the model

This section discusses the geometric models that exhibit negative Poisson's ratio behaviour. Figure 1 illustrates two re-entrant [8] configurations commonly used in auxetic design. The first is the H-shaped re-entrant unit cell [Figure 1(a)], which features a geometry resembling the letter "H". In this design, a central vertical strut connects two horizontal arms that bend inward, forming re-entrant angles [3] responsible for the auxetic effect. H-shaped re-entrant unit cells specimens' size 174x80x4mm, total 12 sets of specimens prepared and simulated. A collection of H-shaped structure is shown in Figure 3.
The second configuration is the double arrow or V-shaped re-entrant unit cell [Figure 1(b)], composed of angled struts that form a "V" shape, with the apex pointing upward within the unit cell. This arrangement also produces auxetic behaviour through its re-entrant geometry. Double arrow or V-shaped re-entrant unit cells specimens' size 174x80x4mm, total 12 sets prepared and simulated. A collection of V-based structure is shown in Figure 3.

The fundamental difference between these two models lies in their symmetry. The H-shaped unit cell exhibits double symmetry, meaning it is symmetrical both horizontally (left-right) and vertically (top-bottom). In contrast, the double arrow or V-shaped unit cell displays single symmetry, being symmetrical only in the horizontal direction. This distinction in symmetry influences the mechanical response and deformation characteristics of each structure [1].
In terms of curved-based structures, this study considers two types of unit cells: the elliptical unit and the peanut-shaped unit [1]. The elliptical unit cell is designed using repeating elliptical shapes arranged both vertically and horizontally, as shown in [Figure 2(a)]. These elliptical elements deform by rotating when stretched [2], which causes lateral expansion and results in a negative Poisson's ratio. Curve based Elliptical unit cells specimens' size 174x80x4mm, total 12 sets prepared and simulated. Each specimen rotated 5-degrees but near the transition zone the degrees increment narrowed down to one decimal to two decimal places to capture the exact transition point of Poisson's ratios. A broader collection of elliptical models is illustrated in Figure 4.
The peanut-shaped unit cell, shown in [Figure 2(b)], features a more complex geometry formed by two connected lobes resembling a peanut. This configuration introduces more pronounced curvature and internal voids, which significantly influence the deformation mechanism [2]. Curve based peanut shaped unit cells specimens' size 174x80x4mm & total specimens prepared 12 sets. Each specimen's unit cells rotated 5-degrees clockwise, near the transition zone the degrees increment lowered to decimal places to capture the actual transition point. A collection of peanut-shaped models is presented in Figure 4.
The key difference between these two geometries lies in their structural complexity. While the elliptical unit cell has a smooth, continuous shape, the peanut-shaped unit cell possesses two distinct lobes at each end. This dual-lobed structure allows for greater geometric variation during deformation [3], potentially enhancing auxetic performance and energy absorption.

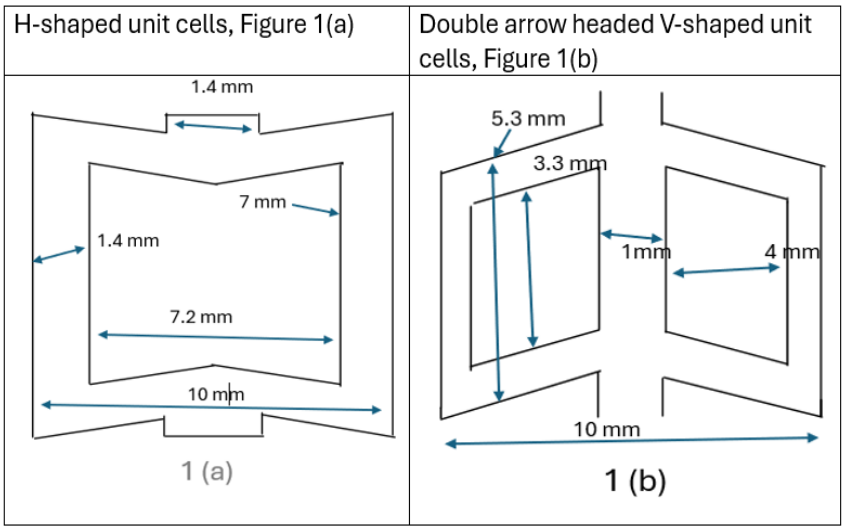

Fig 1. Re-entrant Edge-based two sets of specimens H & double arrow V-shaped unit cells

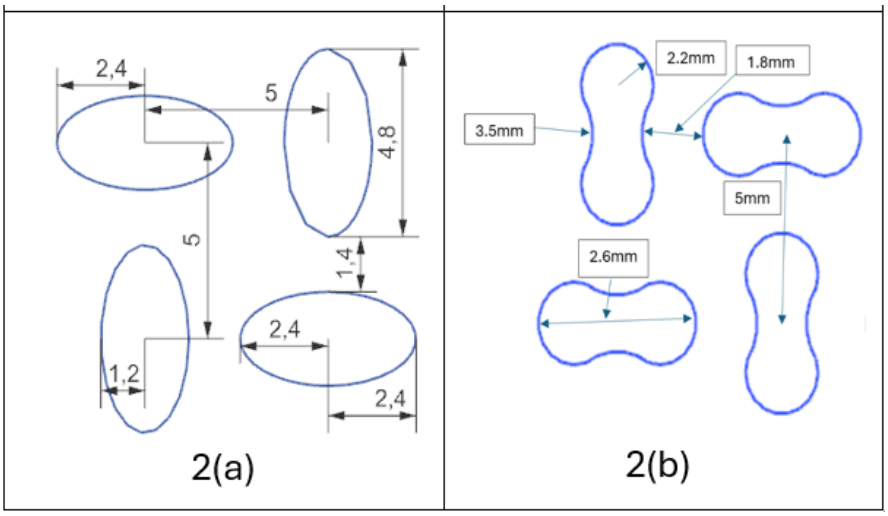

Fig 2. Curve based two sets of specimens Elliptical 2(a) & Peanut shaped unit cells 2(b).

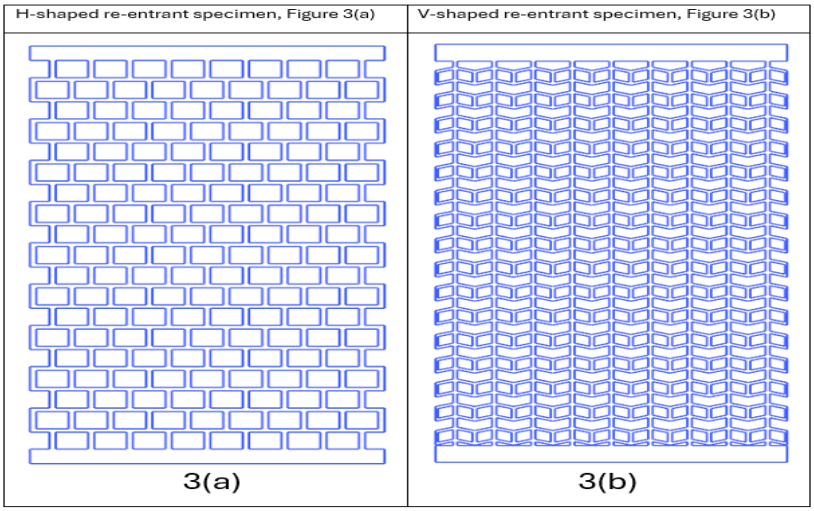

Fig 3. H-shaped 3(a) and double arrow headed V-shaped 3(b)

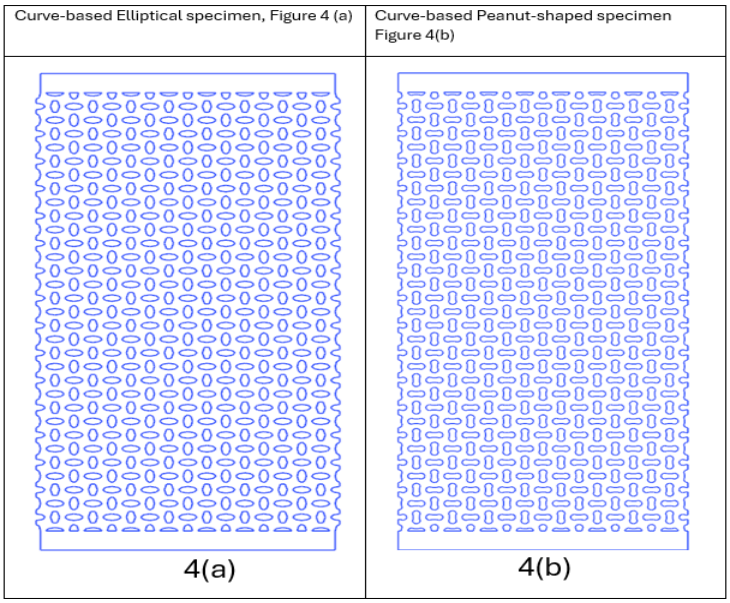

Fig 4. Elliptical 4(a) & Peanut -shaped 4(b) specimen

2 Finite element analysis

The structure is planar and has uniform cross section through the thickness. The loading and constraint are mainly in-plane with negligible out-of-plane stresses [3]. The objective was to capture the in-plane Poisson's ratio or strain fields, not through thickness stresses.

The geometry exhibits planar symmetry and uniform thickness, and the nature of the deformation was primarily in-plane.
The model was discretised using 2D quadrilateral elements under a plane-stress formulation, with a nominal thickness of 4mm assigned to represent the actual specimen section. This approach was adopted because the specimen was (174x80x4mm) and undergoes predominantly in-plane deformation under uniaxial tensile loading [4]. The 2D representation effectively captures the stress and strain distribution within the lattice while substantially reducing computational requirements compared with 3D solid modelling. The uniform thickness assumption is valid as the stress gradients through the thickness are negligible for the present loading configuration.

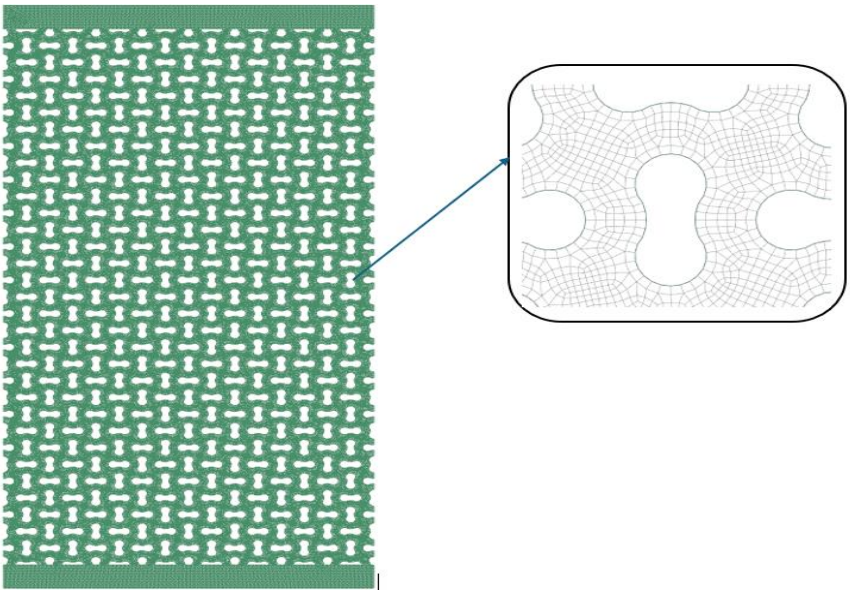

Fig 5. Paver meshing with CQUAD4 element size 0.3mm

3 Reliability of the simulation

Model overview: Four types of specimens were designed with identical dimensions (174x80x4mm), differing only in the internal unit cell geometry. Four types are re-entrant based H-shaped, V-shaped, curve based peanut shaped and elliptical shaped unit cells of 10mm size.

Materials used and properties: Linear-elastic isotropic ABS (Acrynitrile Butadine Styrene) were used to model the specimens with Young's modulus E=2.1 Gpa, Poisson's ratio v=0.35. Similar material parameters were applied across all specimen types.

Boundary conditions and loading setup: The lower edge of the specimen was fully constrained in all degrees of freedom. The upper edge was subjected to uniaxial tensile loading progressively in ten steps with time interval of 2 seconds. All other faces kept left free. Identical loading conditions and constraints were applied across all specimen types to maintain consistency and for direct comparison.

Mesh details & convergence: Each model was discretized using 2D mesh and element type of (CQUAD4). With a mesh size of 0.28mm. Mesh convergence confirmed by comparing stress and strain output for finer meshes, to ensure numerical stability and accuracy. Mesh size progressively refined from 0.2mm to 0.9mm. All the mesh size manually selected and paver meshing method used. For each mesh size maximum Von mises stress was recorded.

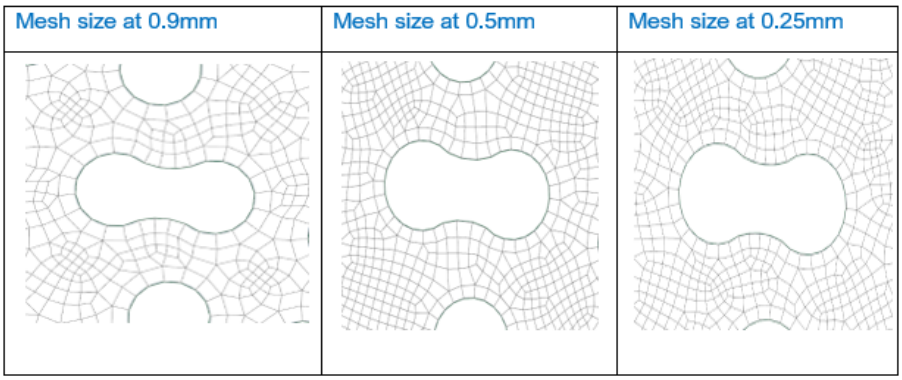

Fig 6. Mesh size.

As the mesh progressively refined the von Mises values gradually stabilized towards convergence. Max. von Mises stress value stabilises between 0.50mm to 0.55mm element size. This shows that further mesh refinement will produce negligible variation in the results.

Table 1. Mesh size, number of elements and von mises stress

Mesh size (mm)	Number of elements	Max von Mises stress
0.90	55668	2.481
0.85	56237	2.504
0.80	68583	2.437
0.75	77514	2.691
0.7	91772	2.615
0.6	107395	2.738
0.55	107921	2.758
0.5	108632	2.758
0.45	109413	2.816
0.4	110419	2.729
0.35	120147	2.85
0.30	124265	2.815
0.28	161322	2.84
0.25	189489	2.91
0.20	306289	3.062

Table 1 shows mesh sensitivity analysis, effect of element size on maximum von mises stress. The relation between mesh element size and the computed maximum von Mises

stress is a major factor for consideration in a finite element analysis. When the mesh becomes finer the element size decreases, the numerical model can represent the geometry and stress distribution with flexibility. This results in an increase in the anticipated max stress values until the solution reaches convergence. Trend and interpretation

- Coarse mesh- (55000-70000 elements)-Stress values are lower (2.48 to 2.69). Large elements cannot capture the local stress concentration accurately. Large size elements simplify the geometry and loading conditions, which tends to flat the stress in gradients and localized stresses peaks hidden.
- Intermediate mesh (90000-160000 elements)- Stress gradually rises to around 2.84 to 2.91 Mpa. Lowering element size improves resolution in critical regions such as fillets, holes, contact interfaces, promotes higher and more accurate stress predictions.
- Fine mesh & convergence (>180000 elements)- Stress increases further and reaches at 3.062 Mpa, then stabilizes. This indicates mesh convergence. Beyond this point further refinement gives only small changes. Once the mesh is sufficiently refined, further reduction in element size produces negligible changes in stress results. This stage indicates that the solution has converged, and the discretization error is minimized.

4 Results and discussion

4.1 Description of re-entrant based h-shaped & double arrow headed v-shaped specimens simulation

Figure 7 illustrates the deformation of the H-shape model as the angle varies from 0° to 30°. At an angle of 0°, when a tensile load of 100 N is applied, the maximum displacement observed is 0.485 mm at the upper part of the model—where the load is applied. In contrast, the lower part shows zero displacement due to the fixed constraint. This indicates a gradual increase in displacement from the bottom to the top, ranging from 0 mm to 0.485 mm. At an angle of 3.5°, under the same 100 N load, the displacement distribution remains similar, following the same pattern of gradual increase from the fixed base to the loaded top. However, at a 30° inclination, the maximum displacement decreases significantly to 0.113 mm under the same load. This reduction suggests a structural transition toward exhibiting a negative Poisson's ratio behaviour as the angle of inclination increases.

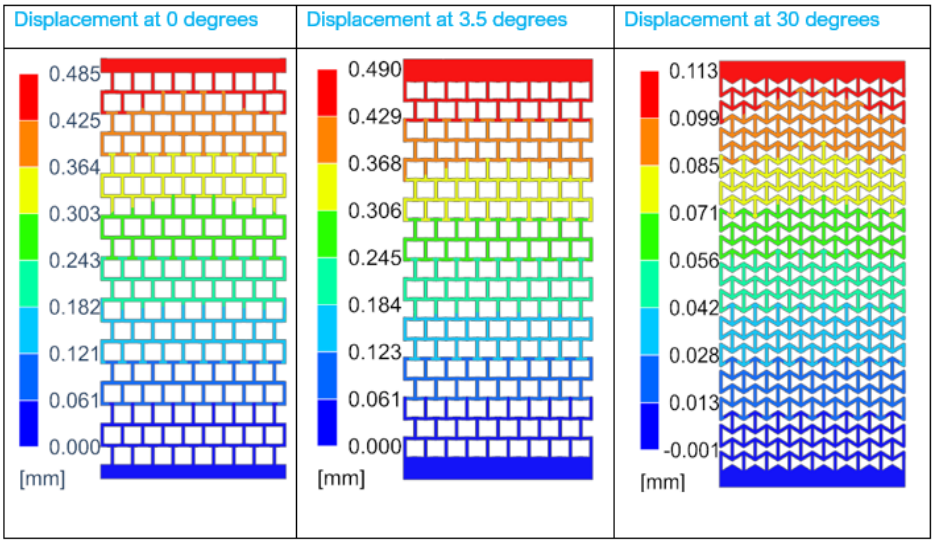

Fig. 7. longitudinal displacement of H-shaped re-entrant unit cells at initial position, near transition and at final position.

Figure 8 represents the transverse displacement distribution of the H-based re-entrant lattice structure under a uniform loading condition of 100 N at three different distinct orientation: 0^0, 3.5^0, and 30^0. These orientations respectively represent the initial configuration, the near-transition zone and the post transition zone of the structure.

At 0^0, the displacement contour indicates a nearly symmetric response about the loading axis, with minimal transverse deformation. This reflects an almost zero Poisson's ratio behaviour, where the lattice neither expands nor contracts in the lateral direction.

At 3.5^0 corresponding to the transition zone, the distribution of displacement begins to deviate from symmetry. Localized regions show both positive and negative transverse displacement values, revealing the onset of deformation mode switching. This intermediate state signifies that the structures transition from non-auxetic to auxetic-like behaviour.

Finally, at 30^0, a pronounced gradient of transverse displacement is observed across the lattice width. The alternating regions of expansion and contraction confirm that the unit cell geometry facilitates directional deformation, characteristics of re-entrant configuration. The clear contrast between the displacement the displacement fields across the three orientations highlights the existence of a distinct transition point, beyond which the lattice exhibits auxetic deformation under the same loading condition.

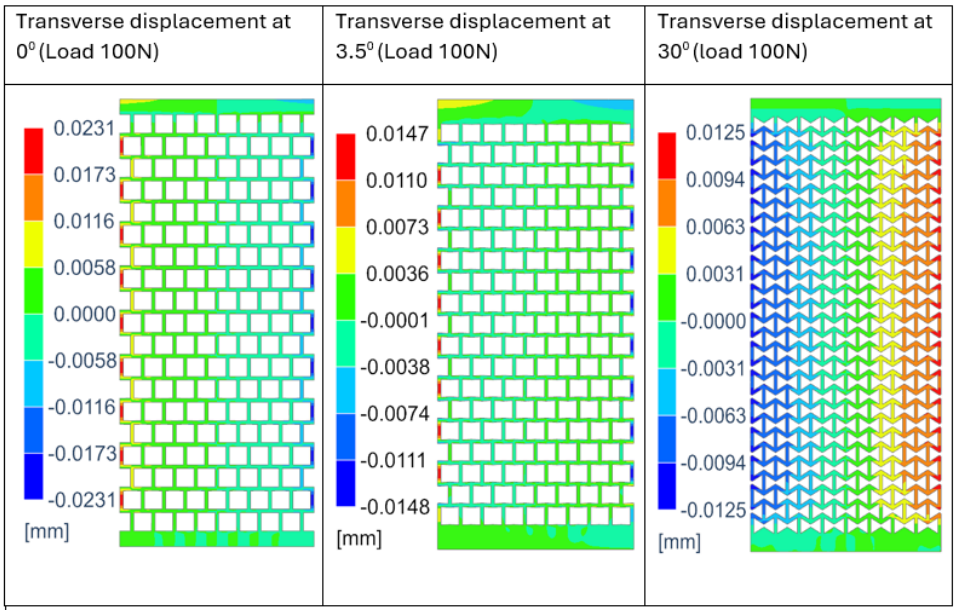

Fig. 8. Transverse displacement of H-shaped specimen

Figure-9 shows that at 100 N load when the strut angles at 0^0 and with positive Poisson's ratio value of 0.2061 the max von mises stress is 6.825 Mpa. At 0^0 the stress is uniformly distributed along the vertical ribs with a maximum of about 6.8 Mpa, indicating axial load transfer and minimal deformation. The behaviour aligns with the non-auxetic regime of the lattice, where the transverse response is negligible.

When the specimen approaches to transition zone at 3.5^0 the stress reduces to 6.445 Mpa. Which represents the transition region. The stress distribution begins to deviate slightly from uniformity. Stress variations near joints and ribs, showing the onset of geometric reorientation and the beginning of the transition region.

At 30^0, transition from positive to negative zone the stress gradually decreases and at 30^0 the stress value becomes 0.961 Mpa. Stress level drops notably and appear more evenly spread, reflecting the auxetic deformation mode where the structure flexes and redistributes the load efficiently. This stress reduction implies that the lattice has entered a fully auxetic deformation mode, where energy is more evenly dissipated through the inclined struts. The decreased stress concentration demonstrates improved load sharing capability and enhanced deformation flexibility at larger rotation angle.

Progressive shifts in stress patterns across the three orientations confirms that the H-based re-entrant structure undergoes a distinct mechanical transition from non-auxetic to auxetic behaviour. The reduction in stress intensity beyond the transition point highlights the structural adaptability and deformation efficiency of the designed lattice under the same applied load.

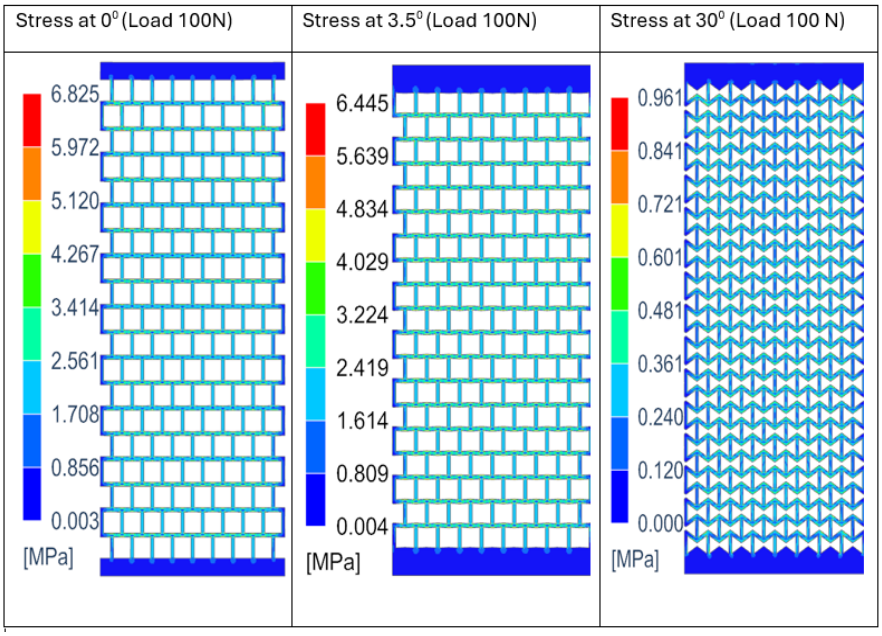

Fig .9. Max von mises stress at initial position, near transition position and at end position.

Figure-10The base configuration corresponds to the specimen with an inner strut angle of 0^0, while subsequent model incorporates a progressive increment of 5^0 in the inward orientation of the strut from both the top and bottom of the unit cells. This gradual geometric modification induces a controlled variation in the mechanical response of the lattice. In the lower angle region (0^0 to 3.5^0). The structure exhibits a positive Poisson's ratio, indicating conventional materials behaviour. As the angle increases, a transition zone is observed between approximately 3^0 and 3.5^0, where the specimen undergoes a distinct shift in deformation mechanism. At this transition point, the material approaches a near zero Poisson's ratio (approx. -0.133) marking a critical change in its lateral deformation response under external loading. This transition reflects the underlying geometric reconfiguration of the H-based re-entrant lattice, which governs its shift from non-auxetic to auxetic like mechanical behaviour.

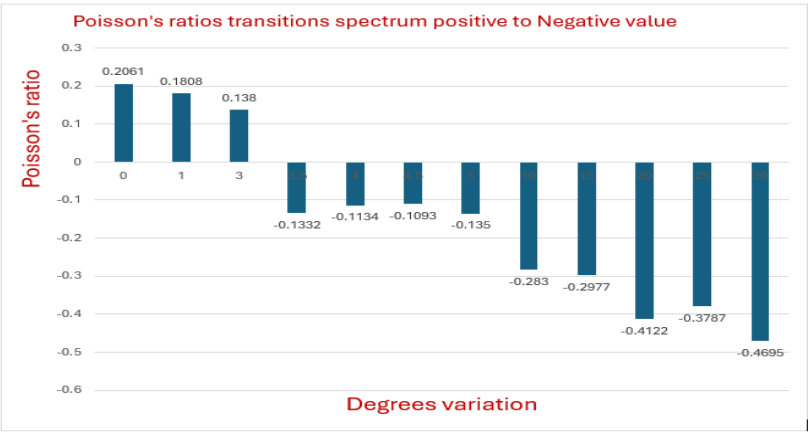

Fig. 10.H-shaped specimens Poisson's ratios transitions from Positive to negative.

Figure-11 illustrates the V-shaped re-entrant specimen deformation behaviour of the V-shaped model as the loading angle varies from 0° to 50°. At 0°, under a tensile load of 100 N, the maximum displacement observed is 0.215 mm at the upper region of the model, where the load is applied. In contrast, the lower region remains stationary due to the fixed boundary condition, resulting in a gradual displacement gradient from 0 mm at the base to 0.215 mm at the top. At an inclination of 19°, the displacement distribution follows a similar pattern, maintaining the progressive increase from the fixed base to the loaded top. However, at a 50° angle, the maximum displacement slightly increases to 0.227 mm under the same loading condition. This behaviour, characteristic of V-shaped re-entrant auxetic structures, indicates minimal variation in longitudinal displacement. The slight increase in axial deformation suggests that the specimen maintains consistent longitudinal stiffness under a 100 N load, while the transverse displacement varies due to the transition from a positive to a negative Poisson's ratio.

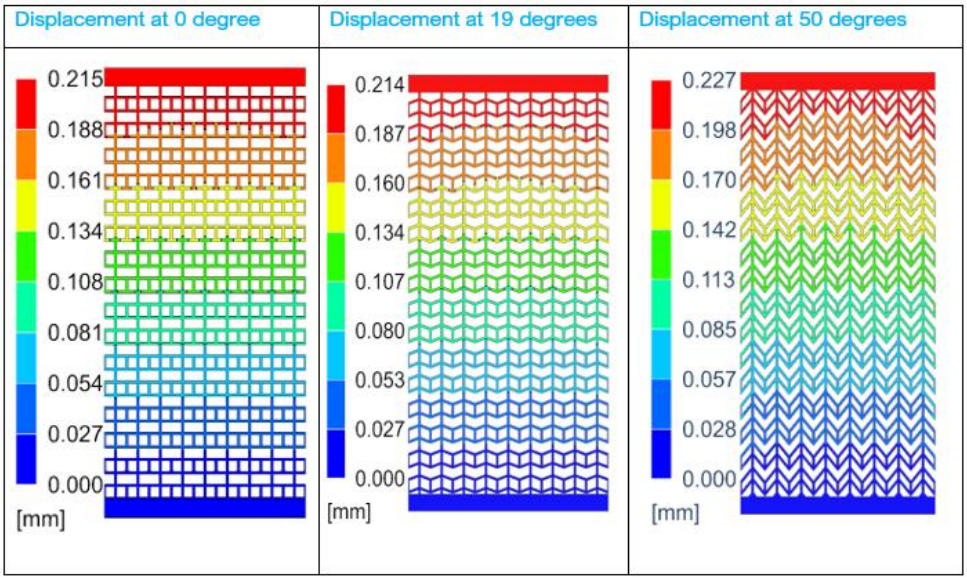

Fig .11. Double arrow headed V-shaped re-entrant specimens displace under tensile load

Figure-12 presents the transverse displacement distribution of the V-shaped re-entrant auxetic structure under a uniform loading condition of 100 N at three distinct orientations, 0^0, 19^0, and 50^0. This orientation respectively represents the initial configuration, the near-transition zone and the post-transition configuration of the structure.

At 0^0, the displacement contour indicates a nearly symmetric about the loading axis, transverse deformation remains minimal. This reflects an almost zero Poisson's ratio behaviour, where the lattice neither expands nor contracts in the lateral direction.

At 19^0, near the transition zone the distribution of displacement shows no significant variations. Localized regions show both positive and negative transverse displacement values, revealing the onset of deformation mode switching. This intermediate state signifies that the structures transition from non-auxetic to auxetic like behaviour.

Finally at 30^0, a significant gradual transverse displacement is observed across the lattice width. The alternating regions of expansion and contraction indicates that unit cells geometry facilitating directional deformation. Transverse displacement across the three orientations highlights the existence of a distinct transition point, beyond which the lattice exhibits deformation under same loading condition.

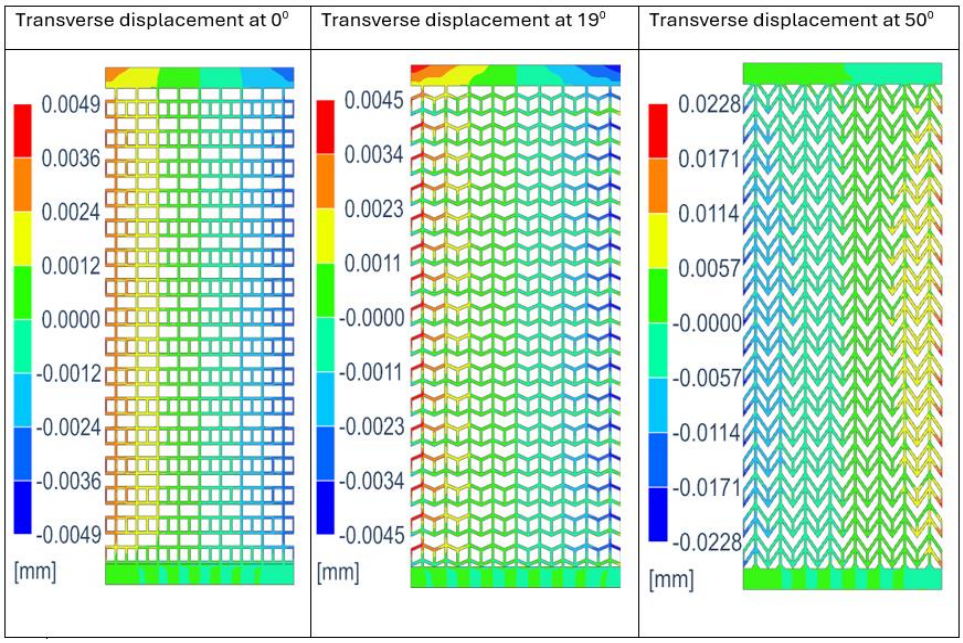

Fig 12. Transverse displacement of double arrow headed V-shaped lattice

Figure-13 presents the variation of von Mises stress in the V-shaped re-entrant lattice model under a tensile load of 100 n as the strut angle increases from 0^0 to 50^0. At 0^0 corresponding to a positive Poisson's ratio of 0.0905, the structure exhibits a maximum von mises stress of 4.179 Mpa, concentrated primarily along the vertical and load-bearing ribs. This indicates that, in the initial configuration, the deformation is dominated by axial stretching, with limited transverse flexibility.

As the angle increases to 19^0, approaching the transition zone, the maximum stress reduces to to 3.684 Mpa, signifying a redistribution of internal forces. The decrease in stress magnitude near this region corresponds to the near-zero Poisson's ratio condition, where the lattice undergoes a mechanical reorientation of its struts. This change allows a more balanced load transfer between the axial and transverse directions, resulting in a lower overall stress concentration.

Beyond the transition zone, as the structure enters the auxetic regime, the von mises stress gradually rises, reaching 4.226 Mpa at 50^0. This increase reflects the re-entrant deformation mode, where the inclined struts rotate inward and contribute to greater local stress concentration despite enhanced lateral expansion.

The stress and inclination angle relationship demonstrates that the minimum stress values occur near the transition region, where the Poisson's ratio approaches zero. In contrast, both the positive and negative Poisson's ratio zones exhibit relatively higher stress levels. This trend confirms that the transition point represents a mechanically critical configuration, characterized by efficient stress redistribution and minimal stress concentration, making the balance between conventional and auxetic deformation response.

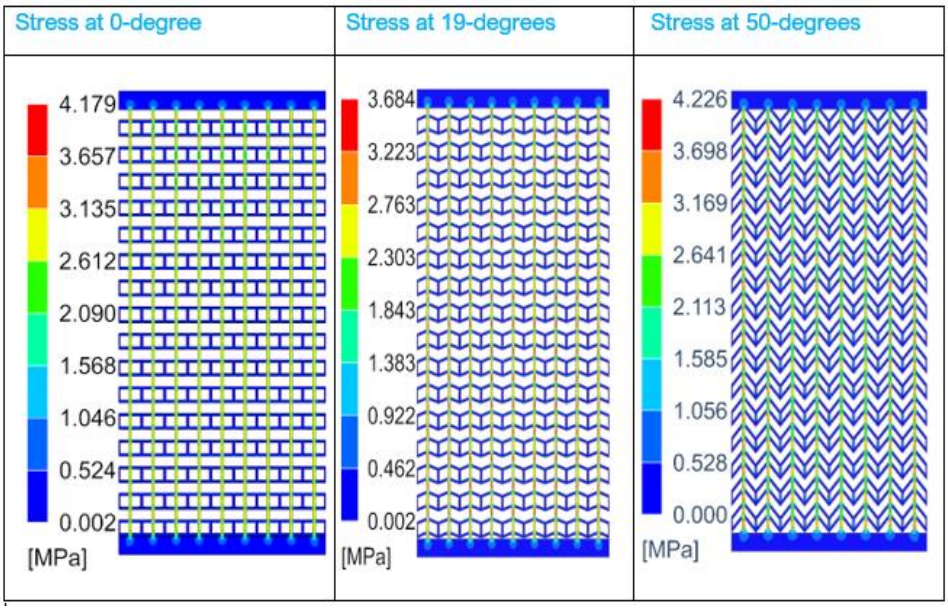

Fig 13. Stress at 3-distinct stages**.**

Figure-14, V-shaped re-entrant specimens' base configuration with an inner strut angle of 0^0, subsequent models incorporate a progressive increment of 5^0, in the upward orientation of the strut angle and increment from bottom of the unit cells. The gradual inclination induces a controlled variation in the mechanical response of the lattice. Between (0^0 to 15^0) the structures exhibit a positive Poisson's ratio, indicating conventional material behaviour, As the angle increases, a transition zone is observed between 15^0 to 19^0, where the specimen undergoes a distinct shift in deformation mechanism. At this transition point, the material approaches, the material approaches a near-zero Poisson's ratio (-0.0816) marking a critical change in its lateral deformation response under external loading. This transition reflects the geometric reconfiguration of the V-shaped re-entrant lattice, struts inclination angle which governs its shifts from non-auxetic to auxetic like mechanical behaviour.

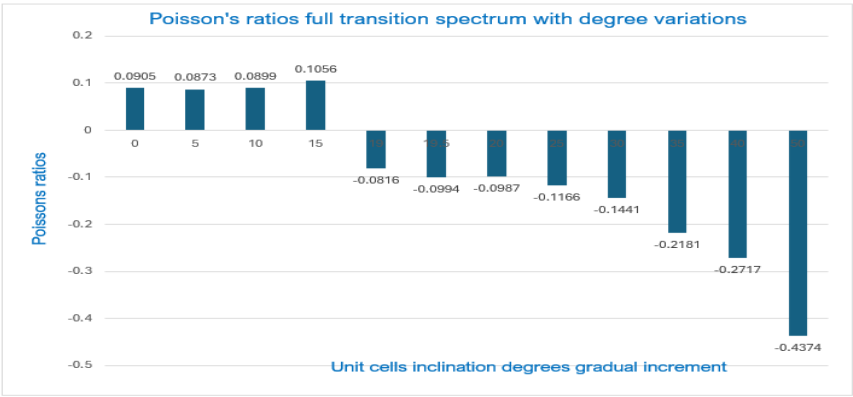

Fig.7. Poisson's ratios transition spectrum (double arrow headed V-shaped specimen)

4.2 Description of curve based elliptical and peanut shaped specimen's simulation explanation

Figure-15 illustrates the longitudinal deformation of the elliptical shaped specimen as the unit cells inclination angle varies from 0^0 to 45^0. At an angle of 0^0 when the tensile load is 100 N, the maximum displacement observed 0.0777mm at the upper part of the model, where the load is applied. Increasing the angle towards 25.45^0 the displacement varies slightly (0.081mm) towards the zero Poisson's ratio zone. Towards 45^0 inclination angle the longitudinal displacement shows almost symmetrical value (0.0695mm). Under the same load of 100N.

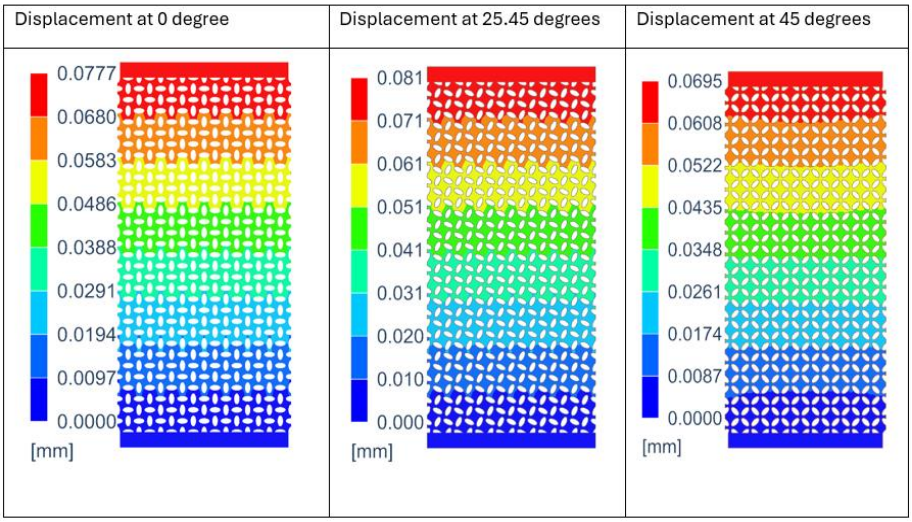

Fig.85 . Longitudinal displacement at 3-stages (Elliptical specimen)

Figure-16 illustrates the transverse displacement distribution of the curve-based elliptical shaped lattice specimen under uniform loading condition of 100 N at three distinct orientations 0^0, 25.45^0, and at 45^0. This orientation respectively represents the initial configuration, near-transition zone and post-transition configuration of the structure. At 0^0, transverse displacement contour indicates a nearly symmetric response about the loading axis. At 25.45^0, the distribution of displacement begins to deviate from symmetry. Localized regions show both positive and negative transverse displacement values. Indicating onset of deformation mode switching. At 45^0, a pronounced gradient of transverse displacement is observed across the lattice width. The alternating zones of expansion and contraction confirms that the unit cell geometry undergoing directional deformation. The displacement field across the three orientations highlights the existence of a distinct transition point, beyond which the lattice exhibits non-auxetic deformation under same loading condition.

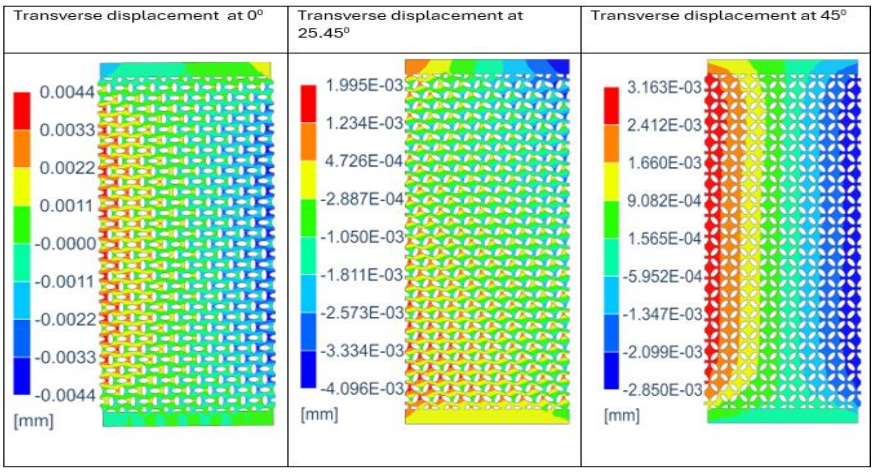

Fig .16. Transverse displacement of elliptical shaped specimens

Figure 17 illustrates the elliptical shaped lattice specimens stress at three distinct orientations. These configurations correspond respectively to the initial state, the near-transition zone, and post-transition zone. At lower degree (0^0-25.45^0) stress contour remains uniform, after the transition zone the stress distribution deviates from the uniformity. The stress magnitude significantly decreases, with a maximum stress of around 1 Mpa. The contour exhibits alternating high and low stress bands towards transverse direction. This stress reduction implies that the lattice undergoes a distinct mechanical transition from auxetic to non-auxetic behaviour [15]. The stress reduction after the transition point highlights the structural adaptability and deformation efficiency of the lattice under the same load.

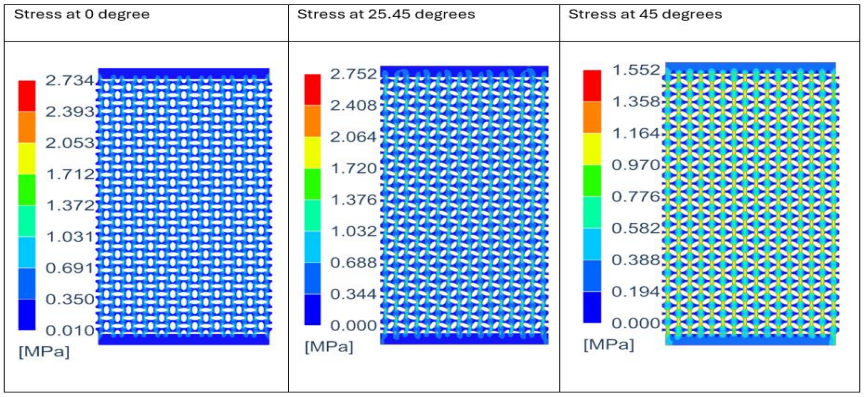

Fig.17. Elliptical specimens von mises stress at 3-load conditions

Figure-18 illustrates the variation of Poisson's ratio in the elliptical shaped lattice specimen, as the unit cell inclination angle increases from 0^0 to 45^0. The trend demonstrates a distinct transition from negative to positivePoissons ratio with increasing inclination angle. At lower inclination angle the (0^0 -25^0) the the Poisson's ratio remains negative and at 25.45^0, the Poisson's ratio reaches its near zero 0.0095. Beyond the transition zone the Poisson's ratio continues to increase gradually to a positive values. The lowest magnitude of Poisson's ratio at 25.45^0, signifies the critical transition zone, where the deformation mechanism changes from auxetic to conventional contraction under tension.

The plot highlights a clear geometric-mechanical relationship, showing that the inclination angle of the unit cells effectively governs the switch between auxetic and non-auxetic responses in the elliptical shaped lattice structures.

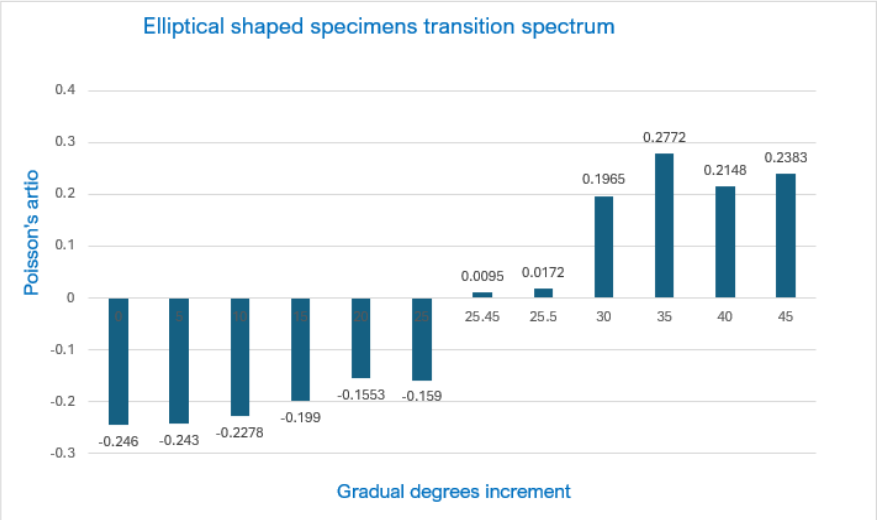

Fig. 18. Poisson's ratios transition spectrum (Elliptical specimen)

Figure-19 Peanut [13] shaped specimen's longitudinal displacement under 3-tensile loading condition. At 0^0, the model exhibits the highest longitudinal displacement of 0.098 mm, with a nearly uniform deformation profile along the loading direction, reflecting dominant axial extension, increasing the inclination angle of the unit cell to 30^0 reduces the displacement to 0.085 mm and introduces a diagonal deformation pattern, indicating improved load distribution and stiffness. At 50^0, displacement further decreases to 0.0776 mm, showing enhanced structural rigidity and efficient stress transfer through the inclined members. Overall, the reduction in displacement with increasing angle highlights the stiffening influence of the geometric orientation.

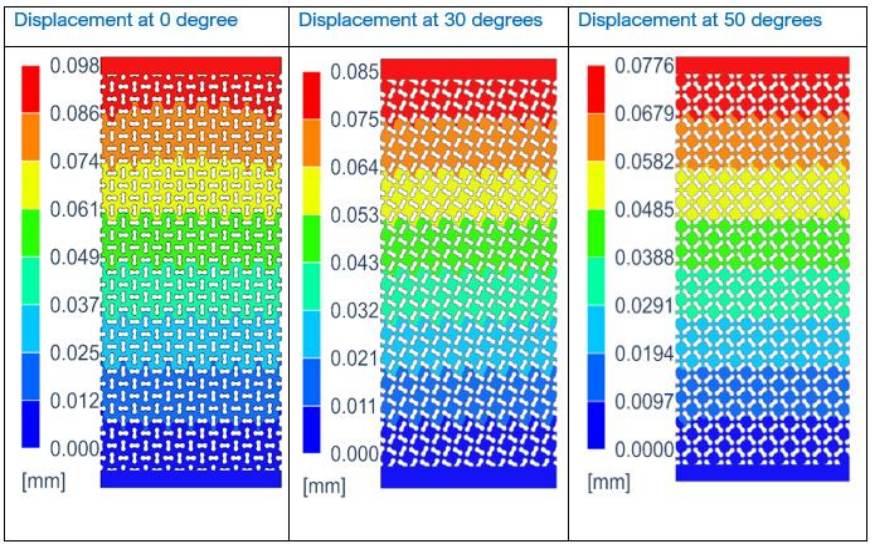

Fig. 9. Peanut shaped specimens displace at 3-stages

Figure-20 Illustrates the transverse displacement distribution of the peanut shaped lattice structure under uniform loading condition of 100 N at three distinct orientations: 00, 300, and 500. At 00, transverse displacement indicates symmetric response about the loading axis. The deformation pattern is auxetic. As the inclination angle increases, at 300, the lattice undergoes transition phase. Near the transition zone the lattice exhibits non - symmetry in transverse displacement, indicating gradual contraction like conventional non-auxetic structure.

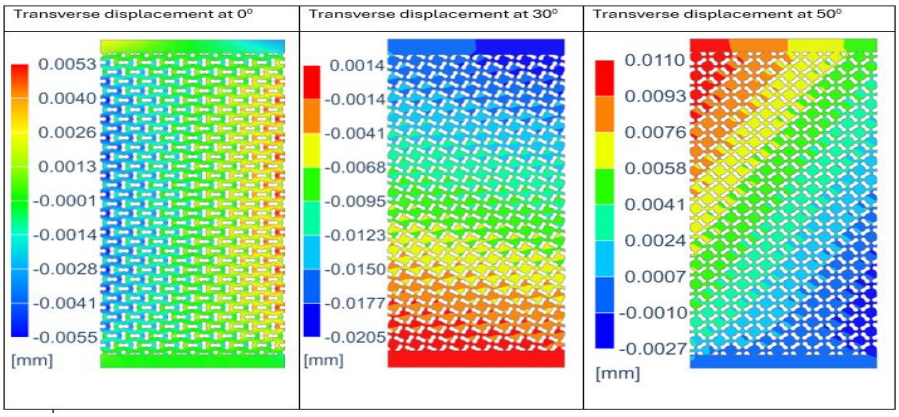

Fig. 20 . Transverse displacement peanut shaped specimen

Figure 21 illustrates Peanut [13] shaped von mises stress at 3-distinct stages. At 0^0, stress is uniformly distributed with higher concentration along the top edge, indicating axial load dominance. At 30^0, slight rotation of stress bands appears, showing diagonal load transfer through inclined ribs and localized stress near the intersections. At 50^0, overall stress magnitude decreases, with a more balanced spread across the lattice, suggesting improved load sharing and reduced localized intensity due to geometric alignment.

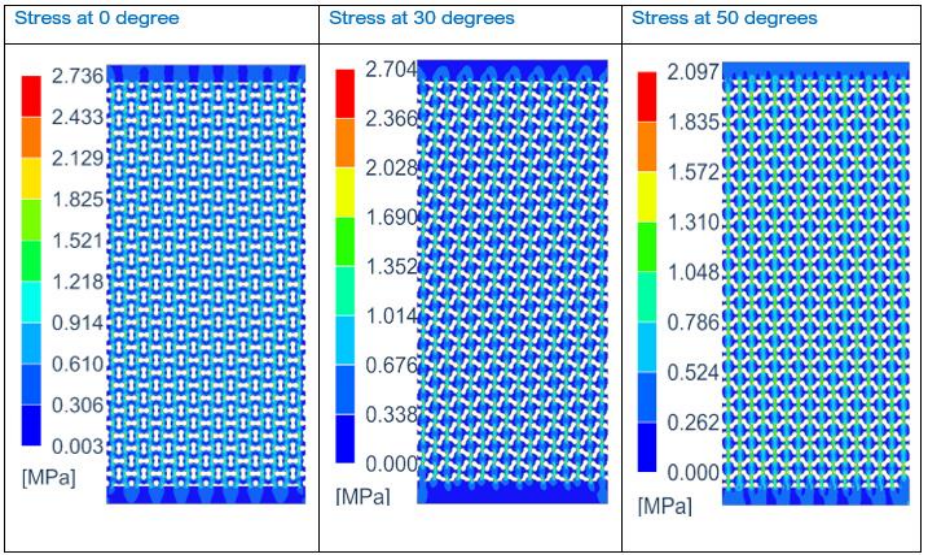

Fig. 21. Von mises stress at 3-stages

Figure 22 illustrates the variation of Poisson's ratio in the Peanut [13] shaped specimen as the unit cell inclination angle increases from 0^0 to 50^0. The trend demonstrates a distinct transition from negative to positive Poisson's ratio with increasing inclination angle.

At lower inclination angle (0^0-30^0), the Poisson's ratio remains negative, reaching its minimum value of nearly -0.5573 at 30^0. This region corresponds to the auxetic phase, where the lattice expands laterally when stretched due to the inward folding of the unit cells [2]. As the inclination increases beyond 30^0, the Poisson's ratio changes sign becoming positive at 35^0, with a value of 0.308.

Beyond the transition point, the Poisson's ratio continues to increase gradually, reaching 0.3847 at 50^0, indicating a complete shift to non-auxetic behaviour. The lowest magnitude of Poisson's ratio around 30^0-35^0 signifies the critical transition zone, where the deformation mechanism changes from re-entrant expansion to conventional contraction under tension [3].

Overall, the plot highlights a clear geometric-mechanical relationship, showing the inclination of unit cells angle effectively governs the switch between auxetic and non-auxetic responses in the peanut [13] shaped lattice structures.

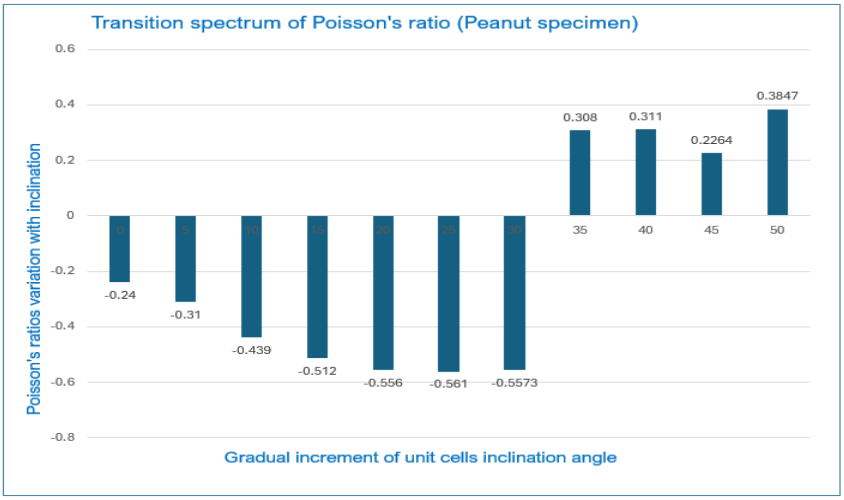

Fig.22. Poisson's ratios transition spectrum (Peanut shaped specimen)

5 Conclusion

This study investigated the influence of geometric configuration on the Poisson's ratio behaviour of four lattice structure types: re-entrant H-based, re-entrant double arrow headed V-shaped, elliptical hole-based, and peanut-shaped hole geometries. By varying the inclination angle in the re-entrant designs and the rotation angle in the hole-based designs, the transition of Poisson's ratio from positive to negative values was examined. Finite element analysis of uniformly manufactured ABS specimens confirmed that the Poisson's ratio response is highly sensitive to these geometric modifications, demonstrating that targeted geometric optimisation provides an effective method for tuning deformation behaviour.

Among the structures analysed, the elliptical hole-based lattice exhibited the most favourable performance for achieving and maintaining a near-zero Poisson's ratio. Its transition occurred smoothly at approximately 25.45°, where the Poisson's ratio reached 0.0095, indicating strong dimensional stability during deformation. The re-entrant H-based and double arrow headed V-shaped structures showed transitions within the negative Poisson's ratio region, displaying gradual and slightly fluctuating behaviours, respectively. In contrast, the peanut-shaped hole structure showed a pronounced and abrupt transition near 35°, shifting quickly from auxetic to positive Poisson's ratio, making it less suitable where stable near-zero behaviour is required.

These results emphasise that inclination angle is a highly controllable and impactful design parameter capable of dictating auxetic behaviour and the position of the Poisson's ratio transition point. Notably, elliptical hole-based geometries allow predictable and smooth tuning around the near-zero Poisson's ratio region, while peanut-shaped and some re-entrant geometries require more precise control due to their sharper transitions.

Overall, this study provides valuable insight into how geometric tailoring enables fine control of lateral deformation characteristics in auxetic structures. The outcomes support the design of multifunctional materials for applications requiring either controlled expansion or lateral dimensional stability, including aerospace structures, biomedical

implants, morphing components, protective devices, and flexible electronic systems. Future work should explore multi-material fabrication and performance under dynamic loading to further expand the applicability of these optimised lattice systems.

References

1. D. Atilla Yolcu, B. Okutan Baba, Measurement of Poisson's ratio of the auxetic structure. Measurement 204, 112040 (2022). https://doi.org/10.1016/j.measurement.2022.112040
2. J.N. Grima, A. Alderson, K.E. Evans, Auxetic behaviour from rotating rigid units. Phys. Status Solidi B 242, 561–575 (2005). https://doi.org/10.1002/pssb.200460376
3. T.-C. Lim, Analogies across auxetic models based on deformation mechanism. Phys. Status Solidi RRL 11, 1700330 (2017). https://doi.org/10.1002/pssr.201770330
4. N. Wang, W. Liu, A. Tang, J. Huang, Z. Lin, S. Lei, Strain isolation: A simple mechanism for understanding and detecting structures of zero Poisson's ratio. Phys. Status Solidi B 251, 2239–2246 (2014). https://doi.org/10.1002/pssb.201451376
5. J. Huang, W. Liu, A. Tang, Effects of fine-scale features on the elastic properties of zero Poisson's ratio honeycombs. Mater. Sci. Eng. B 236–237, 95–103 (2018). https://doi.org/10.1016/j.mseb.2018.11.005
6. K.L. Alderson, K.E. Evans, The fabrication of microporous polyethylene having a negative Poisson's ratio. Polymer 33, 4435–4438 (1992). https://doi.org/10.1016/0032-3861(92)90294-7
7. Y. Li, A review on porous structure negative Poisson's ratio metamaterials. J. Eng. Res. Rep. 27, 189–204 (2025). https://doi.org/10.9734/jerr/2025/v27i11378
8. J. Zhang, G. Lu, Z. Wang, D. Ruan, A. Alomarah, Y. Durandet, Large deformation of an auxetic structure in tension: Experiments and finite element analysis. Compos. Struct. 184, 92–101 (2018). https://doi.org/10.1016/j.compstruct.2017.09.076